

000 001 002 003 004 005 006 007 008 009 010 011 012 013 014 015 016 017 018 019 020 021 022 023 024 025 026 027 028 029 030 031 032 033 034 035 036 037 038 039 040 041 042 043 044 045 046 047 048 049 050 051 052 053 SELECT AND SCHEDULE: AN EFFICIENT HIERARCHICAL OPTIMIZER FOR BLOCKING JOB SHOP SCHEDULING PROBLEM WITH MASSIVE JOBS

Anonymous authors

Paper under double-blind review

ABSTRACT

The Blocking Job Shop Scheduling Problem (BJSP) is a widely studied variant of the classic Job Shop Scheduling Problem. In BJSP, the blocking constraint requires a job to remain on its current machine until the next machine is available. This constraint substantially increases problem complexity, which in turn limits most existing scheduling algorithms to small-scale instances. However, we observe that this blocking constraint also has merit: it naturally restricts the number of jobs processed concurrently, thereby reducing the number of candidate jobs that must be considered at almost any decision point. Building on this insight, we propose a novel hierarchical optimization framework. The higher layer employs a neural network to select a small subset of jobs from a large candidate pool, while the lower layer uses a solver to schedule the selected jobs. Compared with traditional approaches that directly schedule large sets of jobs, our method achieves significantly lower computational complexity and scales almost linearly with the number of jobs. This scalability enables us to efficiently handle larger instances that are previously intractable. Experimental results demonstrate that, on large-scale benchmarks and under comparable runtime budgets, our approach improves solution quality by an average of 11%, while continuing to deliver high-quality solutions within reasonable runtimes for even larger instances.

1 INTRODUCTION

Job-Shop Scheduling Problem (JSP) is a classical and widely studied combinatorial optimization problem with broad applications in manufacturing and automation (Kan, 2012; D’Ariano et al., 2007). Among numerous JSP variants (Li et al., 2022; Mascis & Pacciarelli, 2002), Blocking Job Shop Scheduling Problem (BJSP) is a realistic extension, which frequently encountered in domains such as chemical and pharmaceutical production, food processing, and automated warehousing (Hall & Sriskandarajah, 1996). In BJSP, a set of jobs must be processed on machines, where each job consists of a sequence of operations, each requiring a specific machine and a fixed processing time. Each machine can process only one job at a time. In contrast to classic JSP, BJSP models the more realistic scenario in which no intermediate buffer is available between machines. That is, once an operation completes, if its succeeding machine is not ready, the job remains on the current machine, blocking it from processing other jobs. This blocking constraint makes the problem significantly more complex. The goal is to determine the start times of all operations to minimize the completion time or makespan.

BJSP is further divided into two categories: Blocking No Swap (BNS) and Blocking With Swap (BWS) (Mascis & Pacciarelli, 2002). In BWS, jobs can be temporarily removed to allow others to move, while in BNS, such circular dependencies can cause deadlocks that must be avoided during scheduling. Figure 1 illustrates the specific differences. At time t in BWS, Job 2 on Machine 1 is waiting to move to Machine 2, while Job 3 on Machine 2 is waiting to move to Machine 1. In BWS, it is allowed to simultaneously remove these two jobs from their machines and transfer them to the next machines, making the schedule feasible. However, in BNS, applying the same schedule immediately results in deadlock. Both variants have been proven to be NP-hard (Hall & Sriskandarajah, 1996). Our proposed method is applicable to both BWS and BNS, but the experiments primarily focus on the more challenging BNS case.

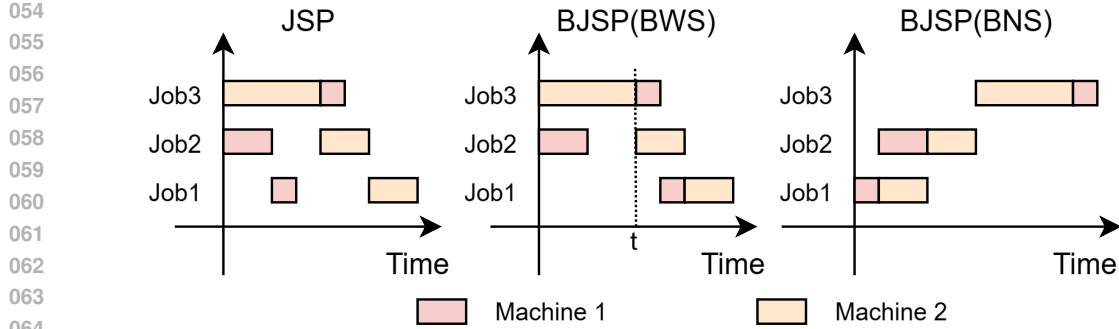


Figure 1: An example schedule for JSP, BNS and BWS. In JSP, Job 1 and Job 2 completed their first operation consecutively, but since Machine 1 is occupied, they wait in the buffer. In contrast, under BWS, when Job 2 finishes an operation, it remains on the current machine, preventing Job 1 from completing its first operation. In BNS, exchange in BWS at time t is not allowed, and consequently its makespan becomes longer.

BJSP is highly challenging, as the blocking constraint drastically increases scheduling complexity. Existing research has mainly followed two directions: exact algorithms and metaheuristics (Dabah et al., 2017; Pranzo & Pacciarelli, 2016; Dabah et al., 2018; Rihane et al., 2022; Lange & Werner, 2019a; 2018). Exact methods can guarantee optimality but become infeasible beyond small instances due to their exponential time complexity (Dabah et al., 2016; 2018; Gmys et al., 2016). Within the class of metaheuristics, tabu search has demonstrated state-of-the-art performance (Lange & Werner, 2018; Mogali et al., 2021; Dabah et al., 2019; 2017). However, it typically requires a large number of iterations to reach high-quality solutions, resulting in relatively high computational cost and making it unsuitable for dynamic or real-time scheduling scenarios.

While the blocking constraint is commonly regarded as a source of computational difficulty, we observe that its inherent restriction on concurrency can be exploited to reduce computational complexity. Specifically, at any given time, the number of jobs that can be simultaneously in process—defined as jobs that have started their first operation but have not yet completed their final operation—is bounded by the number of machines. In high-quality schedules, the number of actively in-process jobs often approaches this upper bound. This implies that, until one of these jobs completes, other jobs typically need not be considered. In other words, in most situations, the scheduler can focus on a small subset of jobs rather than the entire job set.

Building on this insight, we design a hierarchical optimization framework — *Select-and-Schedule* (*S&S*). A high-level neural network dynamically selects a promising subset of jobs from the candidate pool, and a lower-level solver schedules them in detail. This *S&S* framework fundamentally differs from traditional approaches that attempt to schedule all jobs directly. By narrowing the effective problem size at each decision step, our method achieves computational complexity that grows nearly linearly with the number of jobs, making it possible to tackle large-scale BJSP instances that were previously intractable.

We validate our approach on challenging benchmarks and demonstrate that, under comparable run-time budgets, it improves solution quality by an average of 11% over state-of-the-art methods on large instances. Moreover, our framework continues to produce high-quality schedules within reasonable runtimes even as instance sizes grow further, highlighting its scalability and robustness. Our contributions can be summarized as follows:

- We identify a key structural property of BJSP: although the blocking constraint increases scheduling difficulty, it naturally limits concurrency. This observation allows the effective problem size at each decision point to be dramatically reduced, providing a new perspective for scalable scheduling.
- We propose a hierarchical optimization framework *S&S*, which integrates a high-level neural network to dynamically select promising job subsets and a lower-level solver to schedule

108 them. S&S narrows the effective problem size, achieving near-linear computational complexity growth with respect to the number of jobs.
 109
 110

111 • we demonstrates an average improvement of 11% over existing state-of-the-art methods
 112 under comparable runtime budgets. Moreover, S&S maintains high-quality schedules as
 113 problem size increases, highlighting its robustness for large-scale applications.

114 2 RELATED WORKS

115 Mascis & Pacciarelli (2002) conducted one of the earliest comprehensive studies on BJSP, introducing the widely adopted Alternative Graph model as well as a heuristic algorithm. Later work
 116 for BJSP can be broadly divided into exact and approximate methods. Exact methods are primarily based on Branch-and-Bound (B&B). AitZai et al. (2012); Dabah et al. (2018; 2016) attempted
 117 to obtain exact solutions via B&B, further exploring parallel acceleration using physical hardware.
 118 More recently, Rihane et al. (2022) innovatively incorporated learning-based techniques to reduce
 119 search time, where efficient learning of branching and selection strategies significantly sped up the
 120 process, achieving near state-of-the-art performance with substantially fewer search iterations. Al-
 121 though exact methods guarantee optimality, their scalability is severely limited due to the intrinsic
 122 complexity of BJSP, which makes them impractical for real-world scenarios requiring high-quality
 123 solutions within limited computational resources.
 124

125 Approximate methods for the BJSP are mainly based on metaheuristic approaches, which aim to
 126 obtain high-quality solutions without guaranteeing exact optimality. Among these, Tabu Search
 127 (TS) (Glover, 1990) has been the most extensively studied. TS is a local search-based optimization
 128 method that avoids cycling by prohibiting recently visited solutions, thereby escaping local optima
 129 and exploring broader solution spaces. However, unlike JSP, where classical neighborhoods (N1,
 130 NA, NB, N2, N4, N5; (Błażewicz et al., 1996)) are effective, applying them to BJSP tends to yield a
 131 high proportion of infeasible solutions (Mogali et al., 2021). Repairing such solutions incurs signif-
 132 icant computational cost. To mitigate this, Gröflin & Klinkert (2009) attempted to directly construct
 133 feasible neighborhoods, while Dabah et al. (2017) proposed heuristic reconstruction strategies to
 134 improve solution quality. Dabah et al. (2019) further introduced a parallel multistart approach to
 135 accelerate the time-consuming repair process, leveraging 512-core hardware to speed up the search.
 136 More recently, Luo et al. (2021) argued that not all neighbors contribute meaningfully to the search
 137 and developed theoretical insights to reduce complexity, leading to significant efficiency improve-
 138 ments and achieving the first solution for instances of size 100×20. Beyond TS, other metaheuristics
 139 have also been investigated, such as Iterated Greedy, Simulated Annealing, and their variants (Lange
 140 & Werner, 2019a; Pranzo & Pacciarelli, 2016; van Blokland, 2012; Lange & Werner, 2019b). Meta-
 141 heuristics generally produce high-quality solutions on small and medium size instances and benefit
 142 from well-designed heuristics. However, they rely on manually crafted neighborhoods and often
 143 require many iterations, which results in long computational times and limits their scalability and
 144 responsiveness in dynamic or large-scale scheduling scenarios.
 145

146 3 PRELIMINARIES

147 **BJSP** Let $\mathcal{J} = \{1, \dots, n\}$ be the set of jobs and $\mathcal{M} = \{1, \dots, m\}$ the set of machines. Each
 148 job $j \in \mathcal{J}$ is an ordered sequence of operations $\mathcal{O}_j = (o_{j,1}, \dots, o_{j,n_j})$. Operation $o_{j,k}$ requires
 149 machine $m_{j,k} \in \mathcal{M}$ and has processing time $p_{j,k} > 0$. A schedule (solution) is specified by starting
 150 times $S = \{s_{j,k}\}_{1 \leq j \leq n, 1 \leq k \leq n_j}$ with $s_{j,k} \in \mathbb{N}$. The completion time is $c_{j,k} := s_{j,k} + p_{j,k}$. In the
 151 classical Job Shop Scheduling Problem (JSP), once an operation finishes its processing, the machine
 152 is immediately released. In contrast, in the Blocking Job Shop Scheduling Problem (BJSP), no
 153 intermediate buffers are available between machines. Therefore, if the successor machine of an
 154 operation is occupied, the job remains on its current machine after completion, thereby blocking
 155 the machine until the next machine becomes free (Mascis & Pacciarelli, 2002). The size of a BJSP
 156 instance is denoted as $|\mathcal{J}| \times |\mathcal{M}|$. Mathematical formulation about BJSP can be found in A.2
 157

158 **Submodular** Let N be a ground set. Any function $f : 2^N \rightarrow \mathbb{R}$ is called a *set function*. A set
 159 function f is *submodular* if, for any $A \subseteq B \subseteq N$ and any $v \notin B$, it holds that
 160

$$f(A \cup \{v\}) - f(A) \geq f(B \cup \{v\}) - f(B). \quad (1)$$

162 A common problem concerning submodular functions is *Cardinality-Constrained submodular Max-*
 163 *imization* (Nemhauser et al., 1978). Formally, given a submodular function $f : 2^{\mathcal{N}} \rightarrow \mathbb{R}$ and a
 164 cardinality constraint k , the goal is to find a subset $S \subseteq \mathcal{N}$ with $|S| \leq k$ that maximizes $f(S)$:

$$166 \quad \max_{S \subseteq \mathcal{N}, |S| \leq k} f(S). \quad (2)$$

167 Submodular functions exhibit structural properties that allow greedy algorithms to be equipped with
 168 provable and often tight approximation guarantees. A submodular function f is said to be *monotone*
 169 if its value never decreases when elements are added to the set, it holds that:

$$171 \quad f(A) \leq f(B), \quad \forall A \subseteq B \subseteq \mathcal{N}. \quad (3)$$

172 For the problem of maximizing a monotone submodular function subject to a cardinality constraint,
 173 the classical greedy algorithm that iteratively selects the element with the largest marginal gain
 174 achieves a $(1 - 1/e)$ -approximation ratio (Nemhauser et al., 1978). In contrast, for the non-monotone
 175 case, the best-known algorithms currently guarantee a 0.377-approximation ratio (Chen et al., 2024).

177 4 METHOD

178 The iterative procedure of our method is illustrated in Figure 2 and can be divided into three main
 179 stages: Selection, Scheduling, and Schedule Retention. In the Selection stage, a subset of jobs
 180 is chosen from the candidate pool and added to the set of jobs currently in process. During the
 181 Scheduling stage, these in-process jobs are scheduled in detail using the lower-level solver. In the
 182 Schedule Retention stage, a portion of the resulting schedule is preserved, while completed jobs are
 183 removed from the in-process set. This cycle repeats iteratively until all jobs are fully scheduled,
 184 constructing a complete schedule while maintaining a manageable problem size at each step.

185 **Selection Process.** Our method relies on a valuation network to assess whether a group of jobs
 186 exhibits good parallelizability. For instance, in the BNS scenario illustrated in Figure 1, `job1` and
 187 `job2` can partially execute in parallel, whereas `job3` must run serially with `job2`. To quantify
 188 parallelism within a job group, we adopt machine utilization—defined as the total machine
 189 processing time divided by the makespan—as the evaluation metric. This choice is motivated by two
 190 factors: first, maximizing machine utilization directly aligns with our optimization objective, as the
 191 total processing time is fixed and higher utilization implies a shorter makespan. More importantly,
 192 we make the novel observation that the machine utilization of a job set often exhibits approximate
 193 submodular behavior: adding a job to a relatively small set typically increases utilization more than
 194 adding it to an almost full set. This near-submodularity provides a principled abstraction for guiding
 195 our selection process and motivates the application of submodular optimization techniques. Empiri-
 196 cal evidence in Appendix A.4 demonstrates that this property holds in a large proportion of practical
 197 instances, highlighting its practical relevance and validating our approach.

198 During selection, we greedily pick jobs that maximize the total machine utilization at each step.
 199 Selecting k elements from the full set \mathcal{N} to form a subset S that maximizes the set function $f_{\theta}(S)$ is
 200 a challenging problem. However, the submodular property of f_{θ} provides a theoretical foundation
 201 and performance guarantee. In most cases, when S already contains a moderate number of jobs, it
 202 suffices to greedily select a single job a that maximizes f_{θ} :

$$204 \quad a = \arg \max_a f_{\theta}(S \cup \{a\}). \quad (4)$$

205 In other cases, we employ the *Guided Maximal Combinatorial Choice (GMCC)* algorithm (Chen
 206 et al., 2024). GMCC introduces a guided randomized greedy framework that surpasses the $1/e$
 207 approximation barrier for constrained non-monotone submodular maximization. It first applies a
 208 fast local search to construct a *guidance set* Z that captures suboptimal regions, and then runs a
 209 modified randomized greedy algorithm leveraging Z to steer the selection. Detailed algorithmic
 210 steps are provided in the Appendix A.3 and in Chen et al. (2024).

212 **Scheduling** In our framework, we employ a **Constraint Programming (CP) solver** as the sub-
 213 solver to optimize the scheduling of the selected job subset. CP is a widely used paradigm for
 214 combinatorial optimization (Li et al., 2025), which models problems in terms of variables, domains,
 215 and constraints, and efficiently searches for feasible solutions that satisfy all constraints. Using a CP

216

217

218

219

220

221

222

223

224

225

226

227

228

229

230

231

232

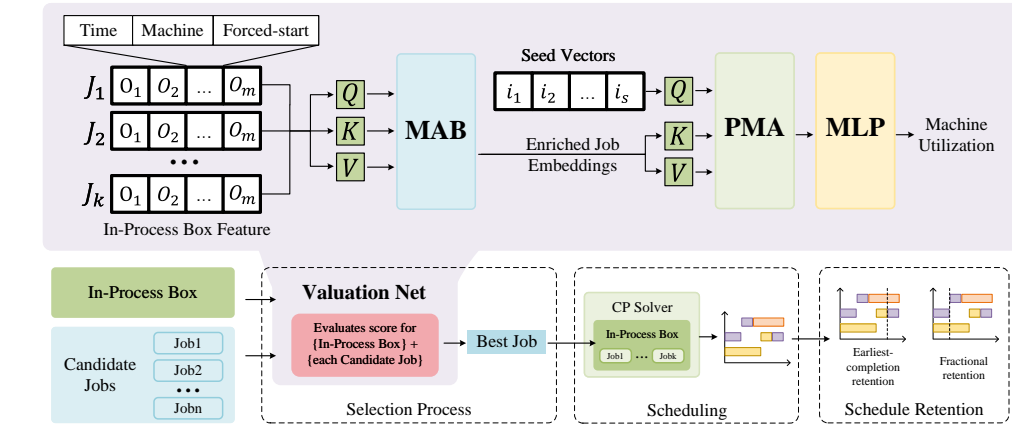


Figure 2: Our hierarchical optimization framework and the detailed architecture of the Valuation Net. The lower panel shows one iteration of our method, which has three main stages. First, in the Selection Process, the Valuation Net evaluates each job in the Candidate Jobs pool, and the job with the highest score is chosen as the Best Job. Second, in the Scheduling stage, this best job is added to the In-Process Box, and the CP Solver then creates a schedule for this complete job subset. Finally, in the Schedule Retention stage, we use a policy to decide which part of the schedule to keep. The upper panel shows the specific structure of the Valuation Net, a Set Transformer model. Input job features are first processed by a Multihead Attention Block (MAB) to capture dependencies between jobs and generate enriched job embeddings. Next, a Pooling by Multihead Attention (PMA) module uses learnable Seed Vectors to aggregate these job embeddings into a fixed-size vector. Finally, this vector is passed to an MLP to predict the overall Machine Utilization.

solver as our subsolver offers several benefits. First, it allows our framework to leverage a mature and general-purpose solver, reducing implementation complexity. Second, CP is highly extensible, which means our framework can be readily adapted to solve variations of the problem, such as the Blocking Job Shop Scheduling Problem with finite waiting times or other practical extensions.

Schedule Retention. At each iteration, we apply a *schedule retention* strategy to decide which portion of the solver-generated schedule σ should be kept and appended to the global solution Π . Concretely, we choose a time τ and retain all operations scheduled before τ , including those already started but not yet completed at τ , while discarding all decisions beyond τ . For truncated jobs, the partially executed operations are treated as already committed: in the next iteration, such operations are forced to start at time 0 on their assigned machines, with their processing times reduced to reflect the portion already executed. Completed operations are removed, and fully finished jobs are discarded. The preserved part σ_{retain} is appended to the global schedule Π , and the remaining subproblem is updated for the next iteration. We proposed two retention strategy : **Earliest-completion retention**. The time point τ is chosen as the earliest completion among all operations in σ . This selection is motivated by the observation that, immediately after τ , the set of in-process jobs is guaranteed to change—often accompanied by the addition of new jobs—making scheduling beyond this point less informative. Moreover, by limiting the schedule to τ , we avoid redundant computations arising from overlapping subproblems at earlier time points, thus improving efficiency. **Fractional retention**. For large-scale subproblems or limited solver budgets, τ is set to a fixed fraction of the earliest completion time. The overlap between consecutive subproblems in our approach is analogous to the rolling-horizon optimization method in Li et al. (2025), allowing repeated subproblem solutions to improve overall quality even when individual solver calls are not optimal.

Network Architecture. To model a set of n jobs, each with m operations, we adopt the **Set Transformer** architecture (Lee et al., 2019). There are two main motivations for this choice. First, we need a network that naturally operates on sets, as the order of jobs should not affect the prediction.

270 Second, the operational features of a single job—the machine IDs of its operations—are often
 271 not meaningful in isolation. Their impact becomes apparent only in relation to other jobs, when
 272 multiple operations require the same machine. Set-based attention allows the model to capture these
 273 inter-job dependencies effectively.

274 Let $x_{jk} = [p_{jk}, m_{jk}, t_{jk}]$ denote the feature vector of the k -th operation of the j -th job where p_{jk}
 275 is the processing time, m_{jk} is the machine ID, and t_{jk} indicates whether the operation is forced to
 276 start. Each operation is embedded as
 277

$$278 \quad \mathbf{o}_{jk} = [\text{Linear}(p_{jk}); \text{Embed}(m_{jk}); \text{Embed}(t_{jk})] \in \mathbb{R}^{d_o}, \quad (5)$$

280 where $d_o = d_p + d_m + d_t$ is the dimension of the concatenated embedding. A learnable positional
 281 encoding $\mathbf{s}_k \in \mathbb{R}^{d_o}$ is added to \mathbf{o}_{ijk} to encode the operation’s position within the job. The embedding
 282 of the j -th is obtained by flattening all m operation embeddings:

$$283 \quad \mathbf{j}_j = \text{Flatten}(\mathbf{o}_{j1}, \dots, \mathbf{o}_{jm}) \in \mathbb{R}^{m \cdot d_o}. \quad (6)$$

285 The n job embeddings form a set $\mathbf{J} = \{\mathbf{j}_1, \dots, \mathbf{j}_n\}$. We pass \mathbf{J}_i through L layers of Set Attention
 286 Blocks (SAB). Each SAB performs multi-head self-attention followed by a feed-forward network
 287 (FFN) with residual connections and layer normalization:

$$289 \quad \mathbf{H} = \text{LayerNorm}(\mathbf{J} + \text{MultiheadAttention}(\mathbf{J}, \mathbf{J}, \mathbf{J})) \quad (7)$$

$$290 \quad \mathbf{J}' = \text{LayerNorm}(\mathbf{H} + \text{FFN}(\mathbf{H})). \quad (8)$$

292 Here, $\text{MultiheadAttention}(Q, K, V)$ denotes the multi-head attention (Vaswani et al., 2017) with
 293 query Q , key K , and value V , and FFN is a two-layer MLP with ReLU activation. This mechanism
 294 allows each job to attend to other jobs in the set \mathcal{J} . After L SAB layers, we aggregate the set into a
 295 fixed-size vector using Pooling by Multihead Attention (PMA):
 296

$$296 \quad \mathbf{z} = \text{PMA}(\mathbf{J}^{(L)}) = \text{Concat}(\mathbf{A}_1 \mathbf{J}^{(L)}, \dots, \mathbf{A}_s \mathbf{J}^{(L)}) \mathbf{W} \in \mathbb{R}^{s \cdot m d_o}, \quad (9)$$

298 where s is the number of learnable seed vectors $\mathbf{S} = [\mathbf{s}_1, \dots, \mathbf{s}_s] \in \mathbb{R}^{s \times d_o}$, and each attention map
 299 is computed as

$$300 \quad \mathbf{A}_i = \text{softmax}\left(\frac{\mathbf{s}_i(\mathbf{J}^{(L)})^\top}{\sqrt{d_o}}\right) \in \mathbb{R}^{1 \times n}. \quad (10)$$

302 Each seed vector attends to all jobs in the set to summarize set-level information, producing $\mathbf{z}_i =
 303 \mathbf{A}_i \mathbf{J}^{(L)}$, and the outputs of all seeds are concatenated and optionally projected by \mathbf{W} . The pooled
 304 vector \mathbf{z} is then mapped to a scalar prediction via an MLP:

$$306 \quad \hat{y} = \text{MLP}(\mathbf{z}) \in \mathbb{R}, \quad (11)$$

307 where \hat{y} denotes the predicted average machine utilization. This design naturally handles variable-
 308 sized job sets, preserves permutation invariance, and captures inter-job dependencies through attention.

311 **Training** We adopt a supervised learning approach using randomly generated BJSP instances.
 312 To simulate realistic scheduling scenarios, we apply two types of perturbations to the job sets: (i)
 313 randomly masking a subset of operations, which mimics partially executed jobs, and (ii) randomly
 314 removing completed jobs. The CP solver is then used to compute supervision labels, defined as the
 315 *machine utilization ratio*, which reflects the degree of parallelism among jobs. For large instances
 316 where the CP solver cannot reach optimality within a reasonable time, we use the best solution found
 317 within a fixed time cutoff as the target. The network is trained to minimize the mean squared error
 318 (MSE) between the predicted and target utilization values.
 319

320 5 EXPERIMENTS

322 Our framework is mainly designed for large-scale BJSP instances. In standard scenarios, inference
 323 follows the three-step procedure described above. However, when the number of jobs is close to
 the number of machines, almost all jobs can be in process simultaneously, making the selection step

324 redundant. In such low-dimensional cases, our method naturally reduces to directly applying the
 325 second schedule-preserving strategy without invoking the network-based selection.
 326

327 We evaluate our proposed framework(S&S) against several baselines on standard benchmarks and
 328 large-scale synthetic instances. More detailed experiments can be found in the appendix A.5. Our
 329 study is guided by these research questions: How well does S&S perform on large-scale BJSP
 330 instances, including extreme sizes? How our proposed framework performs in general scenarios?
 331 How much benefit does the learned selection network provide compared to random or oracle-based
 332 strategies?

333 **Datasets** We conduct experiments on both public benchmarks and synthetically generated in-
 334 stances. Specifically, we evaluate our framework on the Lawrence instances (Lawrence, 1984) and
 335 Taillard instances (Taillard, 1993), which are standard testbeds for job shop scheduling. To further
 336 assess scalability beyond existing benchmarks, we additionally construct larger synthetic instances
 337 using the widely adopted Taillard generation procedure (Taillard, 1993), with sizes reaching up to
 338 (1000, 20). In total, our study spans problem sizes of up to 20,000 operations, substantially extend-
 339 ing the scale considered in prior BJSP research. For comparison, most previous works were limited
 340 to fewer than 600 operations, while Mogali et al. (2021) was the first to give results on instances
 341 approaching 2000 operations.

342 **Baselines** We compare against the following methods: **Tabu Search**: the current state-of-the-art
 343 algorithm for BJSP, employing the $N4/N5$ neighborhood structures (Mogali et al., 2021). This
 344 solver is widely regarded as the strongest heuristic for BJSP to date, and has established the best
 345 known solutions for nearly all benchmark instances considered in our study. **CP Solver**: a widely
 346 used exact solver. **R-S&S**: a variant of our method without the network, where jobs are selected
 347 randomly but with the same selection procedure.

349 **Implementation Details** We describe the experimental setup and hyperparameters used through-
 350 out training. The model employs 16-dimensional embeddings for machines and processing times,
 351 and a 4-dimensional embedding for the forced-start flag. The hidden dimension is set to 64, with
 352 four attention heads and six stacked attention layers. Training instances are generated by perturbing
 353 1,000 randomly created BJSP instances: each job is removed with probability 0.03, and, for surviv-
 354 ing jobs, an operation along with all its predecessors is removed with probability 0.2. The model is
 355 trained for 1,000 epochs with a learning rate of 0.001, using 10% of the data for testing.

356 For synthetic evaluation, 100 instances are generated for each problem configuration, except for very
 357 large instances (500, 20) and (1000, 20), which are limited to 10 instances due to computational cost.
 358 In our hierarchical framework, large-scale problems ($n \geq 50$) use an Earliest-completion retention,
 359 while smaller problems or those where the number of jobs is close to the number of machines employ
 360 a Fractional retention. For the CP solver baseline, subproblems that are too large to solve exactly
 361 are limited to 50 seconds in the unlimited setting. When a global time constraint is imposed, the
 362 allocated time for each subproblem is approximately the total runtime budget divided by the number
 363 of jobs.

365 Table 1: Comparison of Tabu Search and S&S on TA instances

367 Instance	368 Size	369 Tabu 60 Avg Obj	370 S&S 60 Obj	371 Gap (%)	372 Tabu 1800 Avg Obj	373 S&S 1800 Obj	374 Gap (%)
375 TA71	376 100×20	377 17426.6	378 14895	379 -14.53%	380 12369.4	381 12285	382 -0.68%
383 TA72	384 100×20	385 16225.8	386 15763	387 -2.85%	388 11745.6	389 12534	390 6.71%
392 TA73	393 100×20	394 17370.4	395 15313	396 -11.84%	397 12078.6	398 12358	399 2.31%
401 TA74	402 100×20	403 16963.9	404 14788	405 -12.83%	406 12044.8	407 13067	408 8.49%
410 TA75	411 100×20	412 17127.6	413 15151	414 -11.54%	415 11911.4	416 12156	417 2.05%
419 TA76	420 100×20	421 16578.0	422 14774	423 -10.88%	424 12223.8	425 12321	426 0.80%
428 TA77	429 100×20	430 17674.8	431 16365	432 -7.41%	433 12412.2	434 12511	435 0.80%
437 TA78	438 100×20	439 17007.8	440 15014	441 -11.72%	442 11898.6	443 12807	444 7.63%
446 TA79	447 100×20	448 17145.8	449 15834	450 -7.65%	451 12118.4	452 12250	453 1.09%
455 TA80	456 100×20	457 16186.4	458 15100	459 -6.71%	460 11729.0	461 11825	462 0.82%

378 **Results on Benchmark.** Table 1 presents a comparison between our model and the state-of-the-
 379 art Tabu Search on large-scale benchmarks. In our experiments, we considered two scenarios that
 380 correspond to practical settings. The first scenario represents a dynamic environment where a rea-
 381 sonable solution must be obtained within a very short time. We set the runtime limit to 60 seconds.
 382 The second scenario represents a static environment where sufficient but reasonable time is available
 383 to obtain the best possible solution, for which we set the runtime limit to 1800 seconds.

384 Under the 60-second setting, our method achieves consistently better results than the baseline across
 385 all datasets, with an average improvement of 11%, demonstrating the high computational efficiency
 386 of our approach on large-scale problems. Under the 1800-second setting, while our method falls
 387 slightly behind in some cases, in most instances the gap is within 2%, essentially reaching the same
 388 best performance as the state of the art. These results validate both the efficiency and the solution
 389 quality of our method.

390 Table 2 reports the performance of S&S on the small-scale LA benchmark, representing a secondary
 391 scenario where the small problem size reduces the impact of the pre-selection strategy. Overall,
 392 S&S achieves strong early-stage performance: under the 60-second budget, it matches or slightly
 393 outperforms Tabu Search on most instances. With a longer 600-second budget, it generally attains
 394 solution quality comparable to Tabu Search, though in some less favorable instances, a performance
 395 gap remains. These results demonstrate that even in disadvantageous scenarios, S&S maintains
 396 highly efficient early-stage optimization while remaining broadly competitive with state-of-the-art
 397 solvers. Complete results for all instances in Ta and La are provided in Appendix A.5.

399 Table 2: Comparison between Tabu Search and S&S on LA instances

400 Instance	401 Size	402 Tabu 60	403 S&S 60	404 Gap (%)	405 Tabu 1800	406 S&S 1800	407 Gap (%)
408 Avg Obj	409 Obj	410 Avg Obj	411 Obj	412	413	414	415
416 LA01-LA05	417 10*5	418 836	419 836.4	420 0.05%	421 836	422 836.4	423 0.05%
424 LA06-LA10	425 15*5	426 1212.94	427 129.6	428 1.36%	429 1203.4	430 1220.8	431 1.43%
432 LA11-LA15	433 20*5	434 1554.44	435 1569.4	436 0.89%	437 1494.2	438 153.2	439 3.42%
441 LA16-LA20	442 10*10	443 1085.5	444 1082.6	445 -0.26%	446 1082.6	447 1082.6	448 0.00%
451 LA21-LA25	452 15*10	453 1481.5	454 1450.8	455 1.84%	456 1418.8	457 1494.4	458 5.33%
462 LA26-LA30	463 20*10	464 1997.0	465 2075.2	466 5.35%	467 1888.6	468 2060	469 9.08%
474 LA31-LA35	475 30*10	476 2927.32	477 3298	478 12.66%	479 2777	480 3091.8	481 11.34%
487 LA36-LA40	488 15*15	489 1809.2	490 1804.8	491 -0.25%	492 1727.2	493 1767.6	494 2.34%

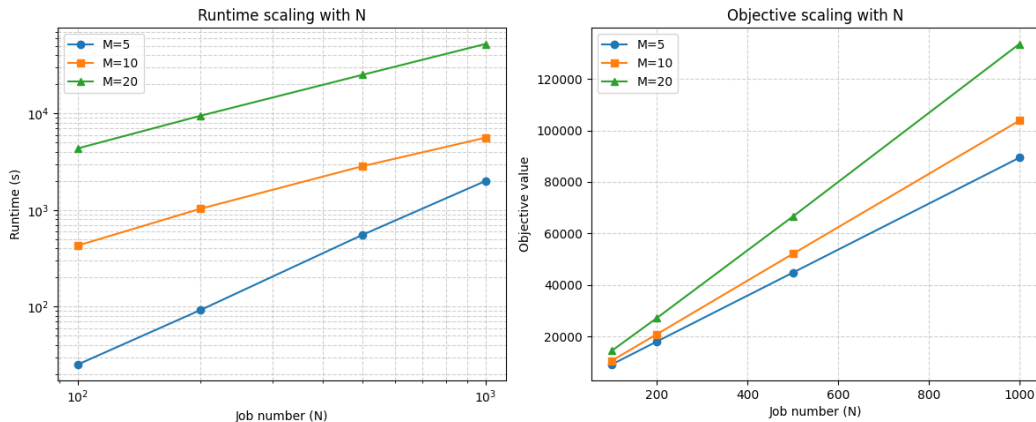
411 Table 3: Comparison of S&S, Random S&S, and CP solver across different problem sizes

413 Mac Num	414 Job Num	415 S&S		416 Random S&S		417 CP solver	
		418 Avg Obj	419 Time (s)	420 Avg Obj	421 Time (s)	422 Avg Obj	423 Time (s)
424 5	425 100	426 9056.1	427 25.2	428 9124.94	429 6.7	430 8660	431 3600
		432 18005.7	433 92.3	434 18162.1	435 12.7	436 27148	437 7200
		438 44752.7	439 555.2	440 45310.7	441 34.3	-	-
		442 89398.1	443 1996.1	444 90380.45	445 74.7	-	-
446 10	447 100	448 10512.2	449 428.7	450 10522.16	451 398.7	452 21473	453 3600
		454 20850.3	455 1031.2	456 20981.1	457 883.4	458 73253	459 7200
		460 52046.9	461 2846.0	462 52088.1	463 2307.7	-	-
		464 103811.2	465 5600.0	466 104032.4	467 3676.8	-	-
468 20	469 100	470 14358.3	471 4340.3	472 14446.8	473 4300.5	474 72135	475 3600
		476 27152.2	477 9447.4	478 27284.4	479 9365.3	-	-
		480 66565.8	481 25103.4	482 66671.8	483 24600.3	-	-
		484 133597.7	485 52293.5	486 134730.5	487 50186.5	-	-

477 **Results on Larger-Scale instances.** Table 3 reports the performance of S&S on large-scale BJSP
 478 instances generated from our production dataset, involving up to 20 machines and 1000 jobs. For
 479 each instance, we compare S&S with the Random S&S baseline, where job subsets are selected
 480 randomly without the valuation network. Across all tested scenarios, S&S consistently achieves
 481 lower objective values than Random S&S. This indicates that the network-based selection effectively
 482 identifies job subsets with higher parallelizability, allowing the solver to produce schedules with

432 better machine utilization. The performance gap between S&S and Random S&S increases with
 433 problem size, suggesting that the network contributes more substantially as the instance grows.
 434

435 On moderately large instances, the standalone CP solver yields worse objective values even with
 436 more computation time, and for the largest instances it fails to produce solutions due to memory
 437 limitations, illustrating the inherent difficulty of BJSP. Notably, our method also employs a CP solver
 438 as the internal optimizer. The performance difference arises because, within the S&S framework, the
 439 CP solver is applied to a carefully selected subset of jobs rather than the full problem. This restricted
 440 formulation substantially reduces the search space, enabling the CP solver to operate effectively
 441 where it would otherwise fail. These results suggest that the strength of S&S lies in the interaction
 442 between learning-based selection and CP optimization, rather than in CP alone.
 443



458 Figure 3: Scaling behavior of our method on synthetic BJSP instances. **(Left)** Runtime grows nearly
 459 linearly with the number of jobs N under different machine settings ($M = 5, 10, 20$). **(Right)** The
 460 obtained objective values also scale linearly with N .
 461

462 To further evaluate the scalability of S&S, we examine the relationship between problem size, run-
 463 time, and solution quality. Figure 3 shows that, for a fixed number of machines, the runtime of S&S
 464 increases approximately linearly with the number of jobs. Correspondingly, the solution objective
 465 also grows roughly linearly with the job count. This linear trend aligns with the intuition that, under
 466 the fixed data-generation distribution, the expected total processing time increases proportionally
 467 with the number of jobs. The observed linear scaling indicates that the computational complexity of
 468 S&S grows moderately with problem size, and that the method remains effective when extrapolated
 469 to very large instances. In contrast, CP solvers fail to produce solutions for the largest instances due
 470 to memory constraints, and their solution quality deteriorates even on moderately sized problems.
 471 These results suggest that S&S maintains both computational efficiency and high-quality schedul-
 472 ing performance across a wide range of problem sizes, highlighting its practical applicability for
 473 large-scale BJSP scenarios.
 474

475 6 CONCLUSION

476 This paper introduces Select and Schedule (S&S), a hierarchical optimization framework for the
 477 Blocking Job Shop Scheduling Problem (BJSP) that scales efficiently to large instances. By ex-
 478 ploiting the observation that blocking constraints limit concurrent jobs to the number of machines,
 479 S&S uses a high-level neural network to select a subset of jobs, which are then scheduled by a
 480 lower-level CP solver. Extensive experiments on standard and large-scale benchmarks show that
 481 S&S consistently produces high-quality solutions. Under tight time constraints (e.g., 60 seconds),
 482 it outperforms state-of-the-art Tabu Search, while remaining competitive with longer time budgets
 483 (1800 seconds). S&S demonstrates robustness and efficiency even for extremely large instances,
 484 offering a practical and scalable solution for real-world dynamic scheduling.
 485

486 REFERENCES
487

488 Abdelhakim AitZai, Brahim Benmedjdoub, and Mourad Boudhar. A branch and bound and parallel
489 genetic algorithm for the job shop scheduling problem with blocking. *International Journal of
490 Operational Research*, 14(3):343–365, 2012.

491 Jacek Błażewicz, Wolfgang Domschke, and Erwin Pesch. The job shop scheduling problem: Con-
492 ventional and new solution techniques. *European journal of operational research*, 93(1):1–33,
493 1996.

494 Yixin Chen, Ankur Nath, Chunli Peng, and Alan Kuhnle. Discretely beyond $1/e$: Guided combi-
495 natorial algortihms for submodular maximization. *Advances in Neural Information Processing
496 Systems*, 37:108929–108973, 2024.

497

498 Adel Dabah, Ahcene Bendjoudi, Didier El-Baz, and Abdelhakim Aitzai. Gpu-based two level par-
499 allel b&b for the blocking job shop scheduling problem. In *2016 IEEE International Parallel and
500 Distributed Processing Symposium Workshops (IPDPSW)*, pp. 747–755. IEEE, 2016.

501 Adel Dabah, Ahcene Bendjoudi, and Abdelhakim AitZai. An efficient tabu search neighborhood
502 based on reconstruction strategy to solve the blocking job shop scheduling problem. *Journal of
503 Industrial & Management Optimization*, 13(4), 2017.

504

505 Adel Dabah, Ahcene Bendjoudi, Abdelhakim AitZai, Didier El-Baz, and Nadia Nouali Taboudjemat.
506 Hybrid multi-core cpu and gpu-based b&b approaches for the blocking job shop scheduling
507 problem. *Journal of Parallel and Distributed Computing*, 117:73–86, 2018.

508 Adel Dabah, Ahcene Bendjoudi, Abdelhakim AitZai, and Nadia Nouali Taboudjemat. Efficient par-
509 allel tabu search for the blocking job shop scheduling problem. *Soft Computing*, 23(24):13283–
510 13295, 2019.

511

512 Andrea D’Ariano, Dario Pacciarelli, and Marco Pranzo. A branch and bound algorithm for
513 scheduling trains in a railway network. *European Journal of Operational Research*, 183(2):643–
514 657, 2007. ISSN 0377-2217. doi: <https://doi.org/10.1016/j.ejor.2006.10.034>. URL <https://www.sciencedirect.com/science/article/pii/S0377221706010678>.

515

516 Fred Glover. Tabu search: A tutorial. *Interfaces*, 20(4):74–94, 1990.

517

518 Jan Gmys, Mohand Mezmaz, Nouredine Melab, and Daniel Tuyttens. A gpu-based branch-and-
519 bound algorithm using integer–vector–matrix data structure. *Parallel Computing*, 59:119–139,
520 2016.

521

522 Heinz Gröflin and Andreas Klinkert. A new neighborhood and tabu search for the blocking job shop.
523 *Discrete Applied Mathematics*, 157(17):3643–3655, 2009.

524

525 Nicholas G Hall and Chelliah Sriskandarajah. A survey of machine scheduling problems with block-
526 ing and no-wait in process. *Operations research*, 44(3):510–525, 1996.

527

528 AHG Rinnooy Kan. *Machine scheduling problems: classification, complexity and computations*.
Springer Science & Business Media, 2012.

529

530 Julia Lange and Frank Werner. A permutation-based neighborhood for the blocking job-shop prob-
531 lem with total tardiness minimization. In *Operations Research Proceedings 2017: Selected Pa-
532 pers of the Annual International Conference of the German Operations Research Society (GOR),
533 Freie Universität Berlin, Germany, September 6-8, 2017*, pp. 581–586. Springer, 2018.

534

535 Julia Lange and Frank Werner. On neighborhood structures and repair techniques for blocking job
536 shop scheduling problems. *Algorithms*, 12(11):242, 2019a.

537

538 Julia Lange and Frank Werner. A permutation-based heuristic method for the blocking job shop
539 scheduling problem. *IFAC-PapersOnLine*, 52(13):1403–1408, 2019b.

540

541 Stephen Lawrence. Resouce constrained project scheduling: An experimental investigation of
542 heuristic scheduling techniques (supplement). *Graduate School of Industrial Administration,
543 Carnegie-Mellon University*, 1984.

540 Juho Lee, Yoonho Lee, Jungtaek Kim, Adam Kosiorek, Seungjin Choi, and Yee Whye Teh. Set
 541 transformer: A framework for attention-based permutation-invariant neural networks. In *International
 542 conference on machine learning*, pp. 3744–3753. PMLR, 2019.

543

544 Sirui Li, Wenbin Ouyang, Yining Ma, and Cathy Wu. Learning-guided rolling horizon optimization
 545 for long-horizon flexible job-shop scheduling. *arXiv preprint arXiv:2502.15791*, 2025.

546

547 Xixing Li, Xing Guo, Hongtao Tang, Rui Wu, Lei Wang, Shiba Pang, Zhengchao Liu, Wenxiang
 548 Xu, and Xin Li. Survey of integrated flexible job shop scheduling problems. *Computers &
 549 Industrial Engineering*, 174:108786, 2022.

550

551 Shu Luo, Linxuan Zhang, and Yushun Fan. Real-time scheduling for dynamic partial-no-wait mul-
 552 tioobjective flexible job shop by deep reinforcement learning. *IEEE Transactions on Automation
 553 Science and Engineering*, 19(4):3020–3038, 2021.

554 Alessandro Mascis and Dario Pacciarelli. Job-shop scheduling with blocking and no-wait con-
 555 straints. *European Journal of Operational Research*, 143(3):498–517, 2002.

556

557 Jayanth Krishna Mogali, Laura Barbulescu, and Stephen F Smith. Efficient primal heuristic updates
 558 for the blocking job shop problem. *European Journal of Operational Research*, 295(1):82–101,
 559 2021.

560

561 George L Nemhauser, Laurence A Wolsey, and Marshall L Fisher. An analysis of approximations
 562 for maximizing submodular set functions—i. *Mathematical programming*, 14(1):265–294, 1978.

563

564 Marco Pranzo and Dario Pacciarelli. An iterated greedy metaheuristic for the blocking job shop
 565 scheduling problem. *Journal of Heuristics*, 22(4):587–611, 2016.

566

567 Karima Rihane, Adel Dabah, and Abdelhakim AitZai. Learning-based selection process for branch
 568 and bound algorithms. In *2022 IEEE Congress on Evolutionary Computation (CEC)*, pp. 1–8.
 569 IEEE, 2022.

570

571 Eric Taillard. Benchmarks for basic scheduling problems. *European journal of operational research*,
 572 64(2):278–285, 1993.

573

574 CHM van Blokland. Solution approaches for solving stochastic job shop and blocking job shop
 575 problems. Master’s thesis, 2012.

576

577

578

579

580

581

582

583

584

585

586

587

588

589

590

591

592

593

594 **A APPENDIX**595 **A.1 USE OF LARGE LANGUAGE MODELS**

598 During the preparation of this work, we employed a Large Language Model (LLM) to polish English descriptions, improving clarity, grammar, and academic style, as well as to provide guidance
 599 in generating text-based prompts for schematic figures, illustrations, and algorithmic diagrams. All
 600 substantive technical decisions, experimental design, core algorithmic code were made by the au-
 601 thors; the use of the LLM served solely as an auxiliary tool to enhance presentation, and visualiza-
 602 tion. We carefully verified the outputs produced with LLM assistance and are fully responsible for
 603 the correctness and integrity of all results and claims presented in this work.

604 **A.2 BJSP MATHEMATICAL FORMULATION**

605 The mathematical formulation of BWS is as follows. These constraints are directly incorporated into
 606 our CP solver, ensuring that both the technological order and machine capacity with blocking are
 607 strictly enforced during the scheduling process.

$$608 \quad s_{j,k+1} \geq s_{j,k} + p_{j,k}, \quad \forall 1 \leq j \leq n, 1 \leq k \leq n_j. \quad (12)$$

$$609 \quad s_{j,k} \geq s_{j',k'+1} \quad \text{or} \quad s_{j',k'} \geq s_{j,k+1}, \\ 610 \quad \forall j, j', 1 \leq j, j' \leq n, 1 \leq k < n_j, 1 \leq k' < n_{j'}, m_{j,k} = m_{j',k'}, j \neq j'. \quad (13)$$

$$611 \quad s_{j,k} \geq s_{j',k'+1} \quad \text{or} \quad s_{j',k'} \geq s_{j,k} + p_{j,k}, \\ 612 \quad \forall j, j', 1 \leq j, j' \leq n, k = n_j, 1 \leq k' < n_{j'}, m_{j,k} = m_{j',k'}, j \neq j'. \quad (14)$$

613 In the above formulation, $s_{j,k}$ denotes the start time of the k -th operation of job j , and $p_{j,k}$ represents
 614 its processing time. The first equation enforces the technological order: each operation must start
 615 only after its preceding operation is completed. The second constraint corresponds to the general
 616 blocking condition: for any two operations sharing the same machine, at least one must start only
 617 after the successor of the other has begun. The third constraint captures the special case where an
 618 operation is the last one of its job; since it has no successor, its completion immediately releases the
 619 machine. The above formulation corresponds to the Blocking No-Wait Shop (BNS) problem. For
 620 the Blocking Job Shop (BWS) problem, Equations (2) and (3) are slightly modified as follows.

$$621 \quad s_{j,k} > s_{j',k'+1} \quad \text{or} \quad s_{j',k'} > s_{j,k+1}, \\ 622 \quad \forall j, j', 1 \leq j, j' \leq n, 1 \leq k < n_j, 1 \leq k' < n_{j'}, m_{j,k} = m_{j',k'}, j \neq j'. \quad (15)$$

$$623 \quad s_{j,k} > s_{j',k'+1} \quad \text{or} \quad s_{j',k'} \geq s_{j,k} + p_{j,k}, \\ 624 \quad \forall j, j', 1 \leq j, j' \leq n, k = n_j, 1 \leq k' < n_{j'}, m_{j,k} = m_{j',k'}, j \neq j'. \quad (16)$$

625 **A.3 GUIDED MULTI-STAGE GREEDY COMBINATORIAL ALGORITHM**

626 The GMGC algorithm (Guided Multi-stage Greedy Combinatorial) is illustrated in Algorithm 1.
 627 The main symbols used are as follows: \mathcal{U} denotes the ground set of elements, $f : 2^{\mathcal{U}} \rightarrow \mathbb{R}$ is the
 628 submodular objective function, \mathcal{I} represents the constraints (e.g., cardinality or matroid constraints),
 629 k is the selection budget, Z_0 is the initial approximate solution, Z is the guidance set generated in
 630 the first stage, A is the solution obtained in the second-stage randomized greedy selection, $t \in [0, 1]$
 631 is the switching ratio controlling the number of initial steps that exclude elements in the guidance
 632 set, and ϵ is the precision parameter used to set the marginal gain threshold during guidance set
 633 construction.

634 In the first stage, the guidance set Z is constructed via the FASTLS subroutine. Elements are it-
 635 eratively added or replaced in Z only if the improvement in marginal gain exceeds the threshold
 636 $\epsilon/k \cdot f(Z)$ and the resulting set satisfies the constraints \mathcal{I} . This process continues until no further
 637 improvement is possible, yielding a guidance set that provides structural information and quality
 638 guarantees for subsequent selection.

639 In the second stage, the GUIDEDRG subroutine performs a randomized greedy selection. During
 640 the first $t \cdot k$ steps, elements from the guidance set are excluded to exploit its structure, while in the
 641

648

Algorithm 1: GMGC (Guided Multi-stage Greedy Combinatorial) Algorithm

649

650 **Input:** Submodular function $f : 2^{\mathcal{U}} \rightarrow \mathbb{R}$, constraint \mathcal{I} , initial solution Z_0 , accuracy ϵ ,
 651 budget k , switching ratio t .

652 **Output:** Final solution S .

653 **1 Phase 1: Guided Set Construction (FASTLS)**654 2 Initialize $Z \leftarrow Z_0$;655 3 **repeat**656 4 **foreach** $a \in \mathcal{U}$ **do**657 5 **if** $a \in Z$ **then**658 6 **foreach** $e \in \mathcal{U} \setminus Z$ **do**659 7 **if** $Z' = (Z \setminus \{a\}) \cup \{e\} \in \mathcal{I}$ **and**660 8 $\Delta(e \mid Z \setminus \{a\}) - \Delta(a \mid Z \setminus \{a\}) \geq \frac{\epsilon}{k} \cdot f(Z)$ **then**661 9 $Z \leftarrow Z'$; **break**;662 10 **else**663 11 **if** $\Delta(a \mid Z) = f(Z \cup \{a\}) - f(Z) \geq \frac{\epsilon}{k} \cdot f(Z)$ **then**664 12 $Z \leftarrow Z \cup \{a\}$;

665

666 13 **until** no improvement;667 **14 Phase 2: Guided Randomized Greedy (GUIDEDRG)**668 15 Initialize $A \leftarrow \emptyset$;669 16 **for** $i \leftarrow 1$ **to** $t \cdot k$ **do**670 17 Compute $\Delta(u \mid A)$ for all $u \in \mathcal{U} \setminus Z$;671 18 Let M_i be the set of top- r elements by marginal gain, where672 $r = \min(k - |A|, t \cdot k - |A|)$;673 19 Pick x_i uniformly at random from M_i ;674 $A \leftarrow A \cup \{x_i\}$;675 20 **for** $i \leftarrow t \cdot k + 1$ **to** k **do**676 21 Compute $\Delta(u \mid A)$ for all $u \in \mathcal{U}$;677 22 Let M_i be the set of top- r elements by marginal gain, where $r = k - |A|$;678 23 Pick x_i uniformly at random from M_i ;679 $A \leftarrow A \cup \{x_i\}$;

680

681 **25 Final Selection:**682 26 Return $S = \arg \max\{f(Z), f(A)\}$;

683

684

685 remaining $k - t \cdot k$ steps, all elements in the ground set are considered. At each step, a candidate
 686 pool is formed by selecting elements with the largest marginal gains, and one element is chosen
 687 uniformly at random to be added to the current solution A . Finally, the algorithm compares the
 688 objective values of the guidance set Z and the greedy solution A , and returns the one with the higher
 689 value as the final output.

690 This two-stage design leverages the high-quality structure of the guidance set while retaining the ex-
 691 ploratory power of randomized greedy selection, achieving strong theoretical guarantees and practi-
 692 cal performance.

693

694 **A.4 SUBMODULAR DISCUSSION**

695

696 As discussed in the main text, the utilization function $F(S)$ is not strictly submodular in all cases.
 697 For instance, consider sets

$$698 \quad A = \{[(1, m_1), (1, m_2)]\}, \quad B = \{[(1, m_1), (1, m_2)], [(1, m_1), (98, m_2)]\},$$

699 and a new job

$$700 \quad c = [(98, m_1), (1, m_2)].$$

701 We have $F(A) = 1$, $F(B) = 1.01$, $F(A \cup \{c\}) = 1.01$, and $F(B \cup \{c\}) \approx 1.98$, so the marginal
 702 gain is larger for the superset B , violating strict submodularity.

702 Nevertheless, we conducted an empirical study to verify that $F(S)$ exhibits approximate submodular
 703 behavior in most cases(t) when the total number of jobs in a set does not exceed the number of
 704 machines m . The experimental procedure is as follows:
 705

- 706 1. Generate random instances of the blocking job shop problem with up to n jobs and m
 707 machines.
- 708 2. For each instance, randomly construct a subset A of jobs with size up to m , and a superset
 709 $B \supseteq A$ with size up to m .
- 710 3. Sample a new random job c .
- 711 4. Solve the scheduling problem for A , B , $A \cup \{c\}$, and $B \cup \{c\}$ to obtain their machine
 712 utilizations $F(A)$, $F(B)$, $F(A \cup \{c\})$, $F(B \cup \{c\})$.
- 713 5. Check whether the marginal gain satisfies

$$714 F(A \cup \{c\}) - F(A) \geq F(B \cup \{c\}) - F(B).$$

- 715 6. Repeat steps 2–5 for a large number of trials (e.g., 10,000) and record the proportion of
 716 cases satisfying the inequality.

717 Based on over 10,000 tests with $m = 5$ and $m = 7$, we find that the utilization function satisfies the
 718 submodularity inequality in the vast majority of cases(almost 100%). This provides strong empirical
 719 support for treating it as approximately submodular in our framework.

720 A.5 DETAIL RESULTS ON BENCHMARK

721 This is all the test results we have on the Ta and La datasets. Table 4 6 reports the full exper-
 722 imental results on the LA and TA benchmark sets, covering instances of varying sizes from small
 723 to extremely large. Overall, our method consistently achieves solutions close to or surpassing those
 724 of Tabu Search across all instances. Under short time budgets , S&S demonstrates a clear advan-
 725 tage, especially on large-scale TA instances, where it rapidly converges to high-quality solutions,
 726 showcasing strong early-stage optimization ability. With longer budgets, S&S remains highly com-
 727 petitive: while Tabu Search occasionally achieves slightly better results on medium-scale cases,
 728 the gap is negligible, and S&S frequently matches or outperforms it. These results confirm that
 729 S&S effectively combines fast convergence with robust scalability, making it not only competitive
 730 with state-of-the-art metaheuristics but also a practical solution for real-world dynamic scheduling
 731 applications.

732
 733
 734
 735
 736
 737
 738
 739
 740
 741
 742
 743
 744
 745
 746
 747
 748
 749
 750
 751
 752
 753
 754
 755

756
757
758
759
760
761
762
763
764

765 Table 4: Comparison between Tabu Search and S&S on LA instances

766 Instance	767 Size	768 60s			769 600s		
		770 Tabu Obj	771 S&S Obj	772 Gap (%)	773 Tabu Obj	774 S&S Obj	775 Gap (%)
776 LA01	777 10*5	778 881	779 881	780 0.00%	781 881	782 881	783 0.00%
784 LA02	785 10*5	786 900	787 900	788 0.00%	789 900	790 900	791 0.00%
792 LA03	793 10*5	794 808	795 810	796 0.25%	797 808	798 810	799 0.25%
800 LA04	801 10*5	802 859	803 859	804 0.00%	805 859	806 859	807 0.00%
808 LA05	809 10*5	810 732	811 732	812 0.00%	813 732	814 732	815 0.00%
816 LA06	817 15*5	818 1203.2	819 1214	820 0.90%	821 1194	822 1194	823 0.00%
824 LA07	825 15*5	826 1132.1	827 1129	828 -0.27%	829 1127	830 1127	831 0.00%
832 LA08	833 15*5	834 1190.2	835 1189	836 -0.10%	837 1173	838 1173	839 0.00%
841 LA09	842 15*5	843 1312.3	844 1311	845 -0.10%	846 1305	847 1305	848 0.00%
850 LA10	851 15*5	852 1226.9	853 1305	854 6.37%	855 1218	856 1305	857 7.14%
859 LA11	860 20*5	861 1588.2	862 1605	863 1.06%	864 1501	865 1590	866 5.93%
869 LA12	870 20*5	871 1414.1	872 1396	873 -1.28%	874 1353	875 1396	876 3.18%
879 LA13	880 20*5	881 1545.6	882 1535	883 -0.69%	884 1508	885 1541	886 2.19%
889 LA14	890 20*5	891 1602.5	892 1637	893 2.15%	894 1544	895 1593	896 3.17%
899 LA15	900 20*5	901 1621.8	902 1674	903 3.22%	904 1565	905 1597	906 2.04%
911 LA16	912 10*10	913 1148.6	914 1148	915 -0.05%	916 1148	917 1148	918 0.00%
919 LA17	920 10*10	921 968	922 968	923 0.00%	924 968	925 968	926 0.00%
928 LA18	929 10*10	930 1082.4	931 1077	932 -0.50%	933 1077	934 1077	935 0.00%
937 LA19	938 10*10	939 1110.5	940 1102	941 -0.77%	942 1102	943 1102	944 0.00%
946 LA20	947 10*10	948 1118	949 1118	950 0.00%	951 1118	952 1118	953 0.00%
956 LA21	957 15*10	958 1556.6	959 1542	960 -0.94%	961 1483	962 1536	963 3.57%
969 LA22	970 15*10	971 1376.2	972 1427	973 3.69%	974 1328	975 1387	976 4.44%
978 LA23	979 15*10	980 1525.2	981 1578	982 3.46%	983 1475	984 1568	985 6.31%
989 LA24	990 15*10	991 1482.8	992 1533	993 3.39%	994 1402	995 1533	996 9.34%
999 LA25	1000 15*10	1001 1466.7	1002 1464	1003 -0.18%	1004 1406	1005 1448	1006 2.99%
1009 LA26	1010 20*10	1011 1980.8	1012 2119	1013 6.98%	1014 1870	1015 2005	1016 7.22%
1019 LA27	1020 20*10	1021 2064.8	1022 2148	1023 4.03%	1024 1933	1025 2170	1026 12.26%
1028 LA28	1029 20*10	1030 2016.7	1031 2127	1032 5.47%	1033 1937	1034 2168	1035 11.93%
1039 LA29	1040 20*10	1041 1898.3	1042 1934	1043 1.88%	1044 1764	1045 1909	1046 8.22%
1049 LA30	1050 20*10	1051 2024.6	1052 2048	1053 1.16%	1054 1939	1055 2048	1056 5.62%
1059 LA31	1060 30*10	1061 2842.8	1062 3347	1063 17.74%	1064 2714	1065 3013	1066 11.02%
1069 LA32	1070 30*10	1071 3106.6	1072 3626	1073 16.72%	1074 2928	1075 3373	1076 15.20%
1079 LA33	1080 30*10	1081 2843.1	1082 3009	1083 5.84%	1084 2717	1085 3009	1086 10.75%
1089 LA34	1090 30*10	1091 2905.7	1092 3072	1093 5.72%	1094 2769	1095 3072	1096 10.94%
1099 LA35	1100 30*10	1101 2938.4	1102 3436	1103 16.93%	1104 2757	1105 2992	1106 8.52%
1109 LA36	1110 15*15	1111 1804.3	1112 1658	1113 -8.11%	1114 1683	1115 1658	1116 -1.49%
1119 LA37	1120 15*15	1121 1929.4	1122 1936	1123 0.34%	1124 1856	1125 1913	1126 3.07%
1129 LA38	1130 15*15	1131 1734.5	1132 1788	1133 3.08%	1134 1665	1135 1704	1136 2.34%
1139 LA39	1140 15*15	1141 1792.2	1142 1792	1143 -0.01%	1144 1720	1145 1792	1146 4.19%
1149 LA40	1150 15*15	1151 1785.4	1152 1849	1153 3.56%	1154 1712	1155 1771	1156 3.45%

803
804
805
806
807
808
809

810
811
812
813
814

Table 5: Comparison between Tabu Search and S&S on TA1-50 instances

Instance	Size	60s			600s		
		Tabu Obj	S&S Obj	Gap (%)	Tabu Obj	S&S Obj	Gap (%)
TA01	15*15	1769.4	1782	0.71%	1761.2	1745	-0.92%
TA02	15*15	1713.6	1808	5.51%	1700.0	1769	4.06%
TA03	15*15	1750.4	1786	2.03%	1715.0	1675	-2.33%
TA04	15*15	1682.6	1855	10.25%	1659.5	1696	2.20%
TA05	15*15	1729.0	1770	2.37%	1712.2	1696	-0.95%
TA06	15*15	1754.4	1829	4.25%	1727.8	1806	4.53%
TA07	15*15	1780.6	1774	-0.37%	1753.6	1797	2.47%
TA08	15*15	1756.6	1830	4.18%	1723.8	1762	2.22%
TA09	15*15	1814.2	1882	3.74%	1797.0	1882	4.73%
TA10	15*15	1762.4	1853	5.14%	1728.6	1853	7.20%
TA11	20*15	2127.6	2164	1.71%	2078.4	2164	4.12%
TA12	20*15	2276.6	2536	11.39%	2228.8	2235	0.28%
TA13	20*15	2134.8	2291	7.32%	2099.0	2165	3.14%
TA14	20*15	2140.2	2330	8.87%	2098.4	2227	6.13%
TA15	20*15	2152.8	2501	16.17%	2106.6	2199	4.39%
TA16	20*15	2236.0	2390	6.89%	2225.6	2236	0.47%
TA17	20*15	2296.0	2761	20.25%	2261.8	2296	1.51%
TA18	20*15	2215.8	2444	10.30%	2157.0	2387	10.66%
TA19	20*15	2190.6	2323	6.04%	2129.4	2316	8.76%
TA20	20*15	2238.6	2382	6.41%	2167.8	2279	5.13%
TA21	20*20	2637.0	2770	5.04%	2517.0	2770	10.05%
TA22	20*20	2536.2	2583	1.85%	2437.0	2583	5.99%
TA23	20*20	2492.6	2771	11.17%	2396.8	2748	14.65%
TA24	20*20	2545.0	2829	11.16%	2484.2	2829	13.88%
TA25	20*20	2487.8	2627	5.60%	2394.4	2575	7.54%
TA26	20*20	2637.2	2784	5.57%	2544.6	2784	9.41%
TA27	20*20	2667.2	2721	2.02%	2577.4	2721	5.57%
TA28	20*20	2545.4	2841	11.61%	2471.6	2835	14.70%
TA29	20*20	2615.2	2744	4.93%	2537.6	2744	8.13%
TA30	20*20	2540.8	2702	6.34%	2465.8	2678	8.61%
TA31	30*15	3358.8	4124	22.78%	3189.0	3453	8.28%
TA32	30*15	3395.4	4336	27.70%	3249.4	3621	11.44%
TA33	30*15	3501.6	3980	13.66%	3362.6	3595	6.91%
TA34	30*15	3474.8	3832	10.28%	3285.2	3832	16.64%
TA35	30*15	3334.2	3575	7.22%	3160.6	3575	13.11%
TA36	30*15	3387.8	3691	8.95%	3270.6	3647	11.51%
TA37	30*15	3478.2	3968	14.08%	3324.8	3652	9.84%
TA38	30*15	3263.2	4406	35.02%	3121.4	3534	13.22%
TA39	30*15	3159.0	3309	4.75%	3036.2	3309	8.98%
TA40	30*15	3270.0	3535	8.10%	3117.4	3535	13.40%
TA41	30*20	3890.4	4036	3.74%	3638.2	4036	10.93%
TA42	30*20	3745.6	3979	6.23%	3535.8	3979	12.53%
TA43	30*20	3618.8	3672	1.47%	3460.0	3672	6.13%
TA44	30*20	3805.0	3967	4.26%	3593.0	3967	10.41%
TA45	30*20	3888.2	4067	4.60%	3578.6	4067	13.65%
TA46	30*20	3867.8	4240	9.62%	3610.2	4240	17.45%
TA47	30*20	3776.0	4239	12.26%	3531.0	4239	20.05%
TA48	30*20	3773.6	3977	5.39%	3513.4	3977	13.20%
TA49	30*20	3694.2	4072	10.23%	3480.8	4072	16.98%
TA50	30*20	3834.2	4067	6.07%	3617.6	4067	12.42%

861
862
863

864
865
866
867
868
869
870
871
872
873
874
875
876

Table 6: Comparison between Tabu Search and S&S on TA51-80 instances

Instance	Size	60s			600s		
		Tabu Obj	S&S Obj	Gap (%)	Tabu Obj	S&S Obj	Gap (%)
TA51	50*15	5689.4	5904	3.77%	5213.8	5904	13.24%
TA52	50*15	5703.8	5794	1.58%	5228.4	5794	10.82%
TA53	50*15	5515.4	5546	0.55%	5113.6	5546	8.46%
TA54	50*15	5540.4	5809	4.85%	5157.4	5809	12.63%
TA55	50*15	5577.4	5765	3.36%	5080.4	5765	13.48%
TA56	50*15	5666.0	5898	4.09%	5233.6	5898	12.69%
TA57	50*15	5731.6	5816	1.47%	5301.4	5833	10.03%
TA58	50*15	5833.0	6076	4.17%	5397.8	6076	12.56%
TA59	50*15	5488.4	5650	2.94%	5108.6	5650	10.60%
TA60	50*15	5757.0	5814	0.99%	5198.0	5757	10.75%
TA61	50*20	6542.6	6774	3.54%	5198.2	6774	30.31%
TA62	50*20	6788.8	6813	0.36%	6021.4	6813	13.15%
TA63	50*20	6441.4	6294	-2.29%	5646.0	6294	11.48%
TA64	50*20	6320.6	6548	3.60%	5576.4	6548	17.42%
TA65	50*20	6512.0	6416	-1.47%	5675.2	6416	13.05%
TA66	50*20	6519.6	6738	3.35%	5816.4	6738	15.84%
TA67	50*20	6567.6	6276	-4.44%	5745.4	6276	9.24%
TA68	50*20	6356.4	6194	-2.55%	5804.2	6194	6.72%
TA69	50*20	6699.6	6580	-1.79%	5907.0	6580	11.39%
TA70	50*20	6764.0	6422	-5.06%	5882.6	6422	9.17%
TA71	100*20	17426.6	14895	-14.53%	12369.4	12285	-0.68%
TA72	100*20	16225.8	15763	-2.85%	11745.6	12534	6.71%
TA73	100*20	17370.4	15313	-11.84%	12078.6	12358	2.31%
TA74	100*20	16963.9	14788	-12.83%	12044.8	13067	8.49%
TA75	100*20	17127.6	15151	-11.54%	11911.4	12156	2.05%
TA76	100*20	16578.0	14774	-10.88%	12223.8	12321	0.80%
TA77	100*20	17674.8	16365	-7.41%	12412.2	12511	0.80%
TA78	100*20	17007.8	15014	-11.72%	11898.6	12807	7.63%
TA79	100*20	17145.8	15834	-7.65%	12118.4	12250	1.09%
TA80	100*20	16186.4	15100	-6.71%	11729.0	11825	0.82%

907
908
909
910
911
912
913
914
915
916
917